J Mater Sci (2007) 42:6729–6734
DOI 10.1007/s10853-006-1474-9

# Macro, micro and nanostructure of $TiO_2$ anodised films prepared in a fluorine-containing electrolyte

**Angkhana Jaroenworaluck · Domenico Regonini · Chris R. Bowen · Ron Stevens · Duncan Allsopp**

Received: 13 November 2006 / Accepted: 19 December 2006 / Published online: 30 April 2007


**Abstract** The paper presents an electron microscopy study of the macro, micro and nanostructure of titania nano-tubes formed by electrochemical anodisation of titanium in a fluorine containing electrolyte. Scanning electron microscopy (SEM) is used to examine the overall structure of the nano-tubes formed under potentiostatic conditions. Transmission electron microscopy (TEM) has been used to examine the structure of the oxide layer of a sample anodised for a relatively short period (30 min) and provides a new insight into the formation of titania nano-tubes. The fluorine ions are able to nucleate sites on the titanium metal and generate a series of interconnected cavities or pores in the oxide complex formed, allowing current to flow within this film. Under specific conditions the cavities and randomly dispersed pores can align in the direction of the applied electric field and link up to generate an array of tubes, where the passage of ions and water is optimised. We also suggest that oxygen evolution at the anode may play a role in the development of the nano-tubes.

A. Jaroenworaluck
MTEC: National Metal and Materials Technology Center, 114 Thailand Science Park, Paholyothin Rd., Klong 1, Klong Luang, Pathumthani 12120, Thailand

D. Regonini (✉) · C. R. Bowen · R. Stevens
Materials Research Centre, Department of Mechanical Engineering, University of Bath, Claverton Down Road, Bath BA2 7AY, UK
e-mail: D.Regonini@bath.ac.uk

D. Allsopp
Department of Electronic & Electrical Engineering, University of Bath, Claverton Down Road, Bath BA2 7AY, UK

## Introduction

Titanium oxide is an interesting and versatile material which is used in many areas of technology, including biomedical [1–3], gas-sensing [4–7], photo-catalysis [8–15], solar cells [16–23] and photonic crystals devices [24]. Anodisation represents a simple and low cost method to synthesise $TiO_2$ by electrochemical oxidation on the surface of a metallic Ti substrate. Previously, production of anodised titania has usually been associated with a decoration process, where colours are generated by an interference effect caused by the thickness of the film. By adding a small amount of hydrofluoric acid or fluorine ions into the electrolyte, nano-sized porosity can be introduced [25, 26] into the oxide morphology and under appropriate conditions titania nano-tubes can be generated [27]. Cavities and pores allow passage of ions through the oxide film [28] and relatively thick layers of $TiO_2$, up to 7 μm in highly viscous electrolyte [29], can be grown. Recently, Paulose and co-workers have grown tubes 134 μm thick by maximising the electrochemical oxidation and controlling the chemical dissolution by reducing the amount of water in their electrolytes [30]. A number of theories, based on field-enhanced dissolution [31, 32] and localised acidification at the base of the pores which increases chemical dissolution [33, 34] have been proposed to explain aspects of the growth mechanism leading to the growth of nano-tubes. The aim of this paper is to provide further insight into the structure of anodised $TiO_2$ films, as generated in a fluorine-based electrolyte using information provided by SEM and TEM. A growth mechanism model involving the rearrangement and linking of cavities in the anodic layer, is proposed. The evolution of oxygen at the anode during our experiments is also discussed as a possible source of the cavities.

Chemistry of the process

The process of formation of anodic oxide appears rather complex, yet a general and simplified model of the chemistry involved is required to understand the process. The outer anodic layer (partly exposed to the electrolyte) has an excess of hydroxyl ions compared to the inner layer [28], and is considered to be $Ti(OH)_4$. The inner layer, where the de-hydroxylation of the film (water releasing) has occurred, is represented as $TiO_2$. In reality there is likely to be a concentration gradient across the film, which can be written as $TiO_2{\cdot}xH_2O$, to represent the inner (dry) and outer (hydrated) anodic oxide.

The reactions which occur at the anode are:

(i) oxidation of the metal which releases $Ti^{4+}$ ions and electrons, Eq. (1):

$$2Ti \rightarrow 2Ti^{4+} + 8e^- \quad (1)$$

(ii) combination of $Ti^{4+}$ ions with $OH^-$ and $O^{2-}$ species provided by the water.

Equations (2) and (3) below account for the hydrated anodic layer and the oxide layer. Further oxide is produced when the hydrated anodic layer releases water by a condensation reaction, Eq. (4):

$$Ti^{4+} + 4OH^- \rightarrow Ti(OH)_4 \quad (2)$$

$$Ti^{4+} + 2O^{2-} \rightarrow TiO_2 \quad (3)$$

$$Ti(OH)_4 \rightarrow TiO_2 + 2H_2O \quad (4)$$

At the cathode there is hydrogen evolution, Eq. (5):

$$8H^+ + 8e^- \rightarrow 4H_2 \quad (5)$$

By summing the equations from (1) to (5), the overall process of oxide formation is given:

$$Ti + 2H_2O \rightarrow TiO_2 + 2H_2 \quad (6)$$

Furthermore, the fluorine ions can attack the hydrated layer and the oxide, as described in the Eqs. (7) and (8), or react with $Ti^{4+}$, Eq. (9), the ions being mobile in the anodic layer, under the high applied electric field [35]:

$$TiO_2 + 6F^- + 4H^+ \rightarrow TiF_6^{2-} + H_2O \quad (7)$$

$$Ti(OH)_4 + 6F^- \rightarrow TiF_6^{2-} + 4OH^- \quad (8)$$

$$Ti^{4+} + 6F^- \rightarrow TiF_6^{2-} \quad (9)$$

Clearly, the competition between formation of the oxide (see Eqs. 2–4) and its dissolution (see Eqs. 7–9), is the key factor in determining the anodic titanium oxide structure produced.

The generation of oxygen at the anode, Eq. (10), has been previously reported as a side reaction during the growth of barrier layer [36] and nano-tubular anodic titania [30]. Based on information provided by our experiments, we suggest it could affect the generation of nano-structured anodic titania, particularly nano-tubes in fluorine containing electrolyte:

$$2H_2O \rightarrow O_2 + 4e^- + 4H^+ \quad (10)$$

## Experimental method

A commercially pure (99.6%) titanium sheet (0.5 mm thick) was used as a substrate. The metal was mechanically polished using SiC, diamond paste (3 μm) and finally a silica suspension (0.02–0.05 μm). Before anodising, the titanium was ultrasonically cleaned in an isopropyl alcohol bath. Anodising was performed under potentiostatic conditions (20 V) or by applying a sweep rate of 100 mV/s before holding the potential at 20 V. Using a Teflon electrochemical cell, 1 $cm^2$ of the metal surface was exposed to the electrolyte (1 M $Na_2SO_4$ + 0.3÷1% wt. of NaF) at the anode, while platinum mesh was used as a counter electrode (cathode). The electrolyte temperature was held constant at 20 °C, without stirring.

The anodised specimens were examined in a SEM (JEOL JSM6480LV) at 30 kV and for higher resolution in a Field Emission SEM. Cross sectional images of the titania layer were obtained after mechanically removing the film from the surface. Fracture of the titania layer also allowed examination of the titanium substrate beneath the oxide layer and examination of the base of the oxide layer. TEM (JEOL JEM2010) samples were prepared from the films of the anodised sample by detaching the oxide film and mounting it in a double layer 200mesh copper grid and observing it directly at 200 kV. The film was further thinned by a focussed ion beam thinning unit (Precision Ion Polishing System, PIPS, Model 691 USA). The conditions used are provided in Table 1.

## Results and discussion

Figure 1 shows a variety of SEM images of the titania nano-tubes obtained in aqueous $Na_2SO_4$/NaF electrolyte. To obtain a well-defined layer of anodised titania nano-tubes, an anodisation time equal or greater than

**Table 1** The sequence of conditions for thinning of the $TiO_2$ anodised film by focussed ion beam thinning

| Ion beam angle (degrees) | Ion gun potential (keV) | Time (min) |
|---|---|---|
| 4 | 4 | 4 |
| 3 | 4 | 6 |
| 3 | 3 | 18 |
| 3 | 2.5 | 8 |

90–120 min was needed. The diameter of the tubes, Fig. 1a and b is approximately 100 nm, in agreement with values reported in literature when applying 20 V [37]. The cross sectional view, Fig. 1c, shows a well-defined array of nano-tubes with a length of approximately 0.8 μm. This is the maximum layer thickness we could obtain at 20 V, even after extending the anodisation time up to 5 h. The use of a voltage ramp before holding the voltage at constant value, lead to the generation of anodic nano-tubes, approximately 1.5 μm thick, as discussed elsewhere [38]. Figure 1d shows the nano-tube layer and the underlying metallic substrate, which is visible where the tubes have lifted off and is formed by a series of concaves. At higher magnification, a cross sectional view of the tubes, Fig. 1e, reveals the presence of a stack of rings which composes the anodic structure, with some broken. The rings are aligned and normal to the metal surface, resulting in the anodised titania nano-tubes. Finally, the scalloped bottom surface of the tubes, which complement the concaves imprinted into the metal substrate, is visible in Fig. 1f. The tubes are clearly closed at the bottom.

In order to investigate the relatively early stages of the growth process, a sample was anodised at 20 V for 30 min and examined in the TEM. The TEM micrographs, Figs. 2 and 3 reveal that the film structure consists not of well-defined tubes as in Fig. 1, but of a series of interconnecting spheroidal cavities or pores, with a high degree of contiguity. Figure 3a provides an insight of the structure which occurs before the pores link-up to generate larger elongated cavities and ultimately tubes. The oxide film has an interconnected porous structure where the ion channels link through the cavities to compete for the total current available. Only those where the current flows above a critical value [28], such as larger channels generated by cavity junctions, will survive. The diffraction pattern (inset Fig. 2) demonstrates that the film at this stage is amorphous.

## Growth mechanism model

Figure 4 represents a schematic view of the possible growth mechanism, based on information obtained by SEM and TEM. In its virgin state, the surface is covered by a thin layer of natural oxide ($TiO_2$). When a voltage is applied, due to the high electric field [35], positive ions such as $Ti^{4+}$ move outward from the anode while negative ions ($O^{2-}$, $OH^-$ and $F^-$) are driven inward into the thin oxide layer to reach the anode, Fig. 4a. For this reason, the growth of the anodic layer can take place at both the metal/oxide and oxide/electrolyte interfaces (Eqs. 1–3).

The anodised layer, when formed, has a certain degree of hydration, as previously reported [28]. The presence of

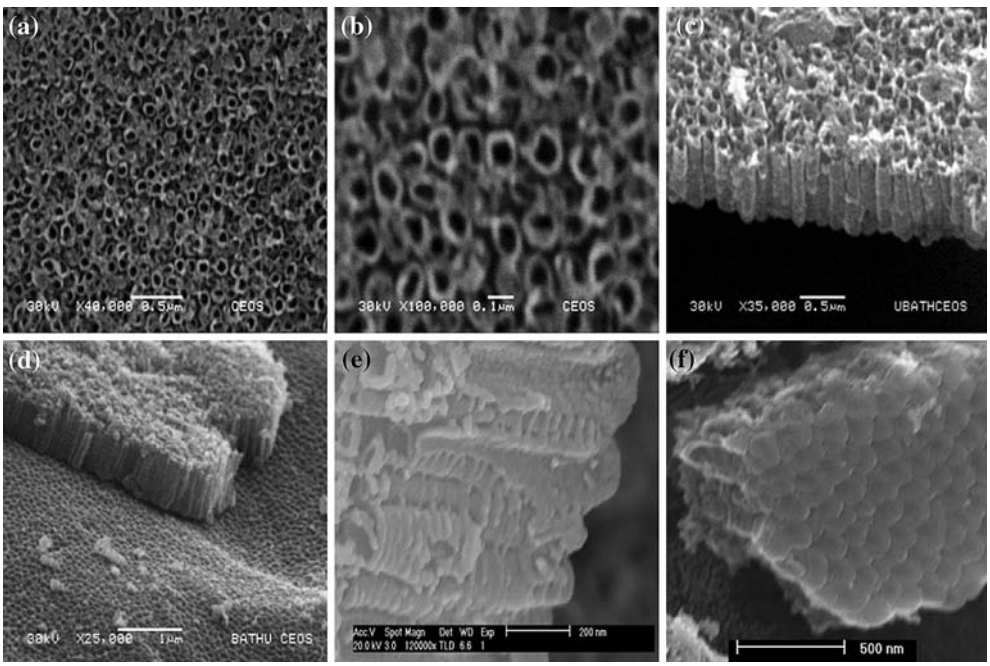


**Fig. 1** SEM images of anodised titania nano-tubes prepared under potentiostatic condition (20 V) in 1 M $Na_2SO_4$/0.5 wt.%NaF. Anodising time ranged from 1 h 30 min to 5 h. (**a**) lower and (**b**) higher front view magnification of the nano-tubes. (**c**), (**d**) and (**e**): cross sectional view of the tubes; in (**d**) the morphology of the Ti, consisting in a series of concaves, can also be seen while in (**e**) the tubes results to be made up by a pile of rings; (**f**) bottom view of the tubes showing their scalloped and closed morphology

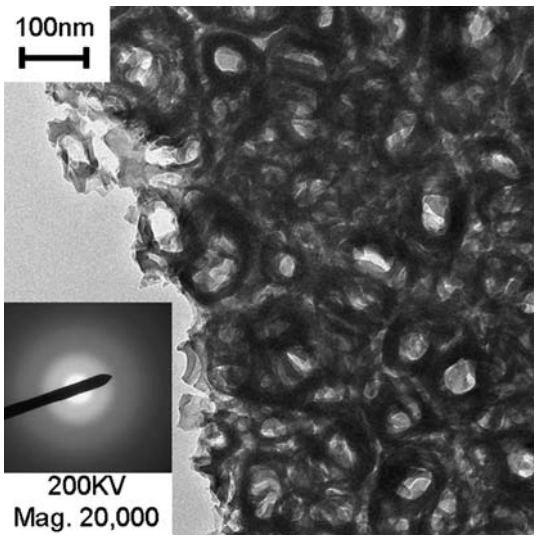


**Fig. 2** TEM micrograph at low magnification showing the macro-structure of the anodised $TiO_2$ film. The corresponding diffraction pattern is shown in the inset

fluorine ions in this the anodic layer can cause etching and generation of cavities, Fig. 4b, which could have a certain mobility in the film, especially, prior to dehydroxylation. The anodic layer can evolve and become thicker, Fig. 4c, because of the high electric field which causes ionic motion. The cavities which will contain liquid and ionic species act as a channel for ionic flow would concentrate in the larger arrays due to lower localised resistance. Under the action of the electric field, cavities would tend to orient vertically to the surface of the metal (i.e. in the direction of the electric field), and to link together, breaching cavity walls to optimise the passage of the current, Fig. 4d. The collapse of part of the linking cavity wall will produce longer channels (normal to the surface, in the direction of the electric field), where resistance is lowered and ions can flow more easily [28]. As a result, the anodic oxide will develop as a series of nano-tubes normal to the metal substrate as described schematically in Figs. 4e and f. The thickness of the tubular layer ceases to increase once the chemical dissolution rate of the oxide at the oxide/electrolyte interface becomes equal to the rate of inward movement of the metal/oxide interface [30, 32]. A 3D perspective of the tubular structure is presented in Fig. 4g. The tubes are shown as an elongated stack of rings, as illustrated in the SEM picture previously discussed. These rings are formed by the anodic layers developed and dehydroxylised (Eq. 4) sequentially. Clearly, as fresh layers are exposed to the film-electrolyte interface they will become more hydrated than the inner layer previously formed, where trapped and adsorbed water can be released into the cavities by condensation reactions.

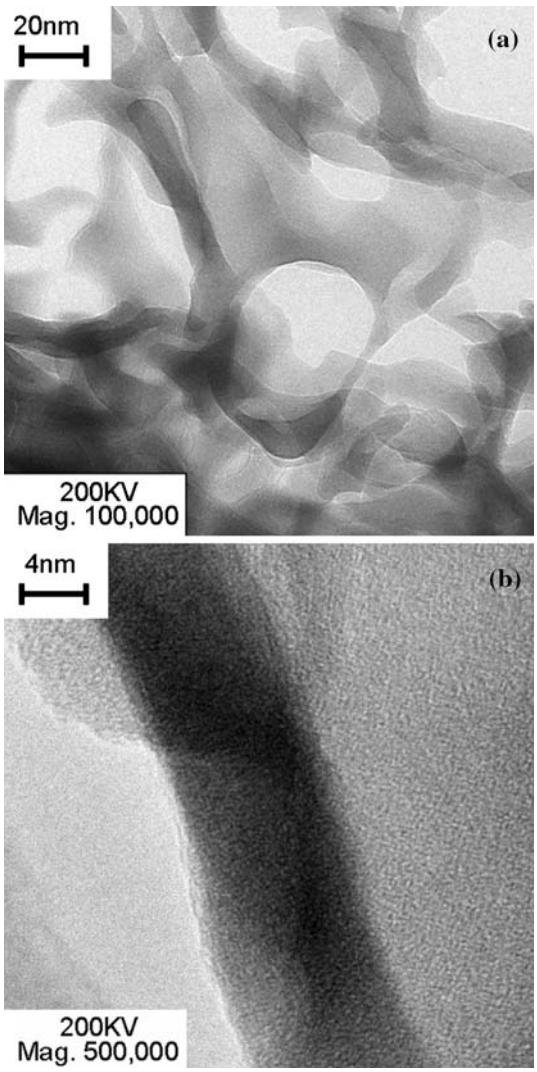


**Fig. 3** TEM micrographs of the fine structure of the pore walls, (**a**), and the structure of the amorphous titanium oxide, (**b**), which make up the walls

The presence of these rings, and the evolution of gas bubbles at the anode (Eq. 10), as observed during certain experiments, also suggests that oxygen evolution itself may play a role in the expansion of the cavities and generation of nano-tubes. The evolution of oxygen by water electrolysis in anodised $Ti/TiO_2$ systems has been previously reported [30, 36]. In the case of anodisation of titanium in fluorine-based electrolyte, oxygen may evolve into the cavities from water trapped into the anodic film/gel. The rings would result from the relatively high internal pressure of the bubbles. Each cavity would be ''constrained'' by neighbouring cavities wall, and the only way to release gas would be on the free surface of the structure (i.e. film-electrolyte interface). This process would contribute to the collapse of the cavities and the development of the tubes (channels). The value of the critical current [28] necessary

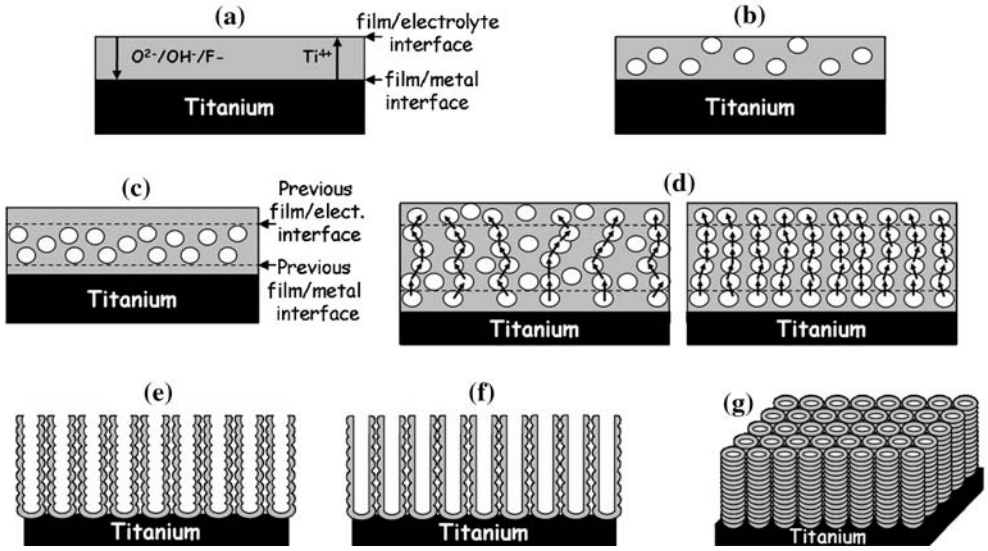


**Fig. 4** Schematic view of the possible growth mechanism. Anodic layer forms because ions are mobile under the high electric field applied (**a**); the presence of fluorine ions generate cavities (**b**) while oxide evolves and becomes thicker (**c**). Under the action of the electric field, cavities would tend to orient vertically to the surface of the metal (i.e. in the direction of the electric field), and to link together (**d**) developing as a series of nano-tubes normal to the metal substrate (**e**) and (**f**). A 3D perspective of the tubes, shown as an elongated stack of rings, is also reported (**g**)

for creating extended channels by pore link up is related to the applied voltage, as well as to the fluoride ionic concentration. In order to create an ordered array of nano-tubes rather than pores, the voltage has to be higher than 3–5 V [27, 37] and fluorine concentration between 0.3 and 1 wt.% [38]. Without the provision of a specific voltage and a specific fluorine concentration, a significant number of pores will cease to grow.

TEM characterisation

As previously stated, Fig. 3 shows the morphology of a film anodised for 30', before the formation of a well-arranged array of nano-tubes. The very fine structure is shown in Fig 3b, and is seen to be non-crystalline, but does have a ''spotty'' appearance and with some indication of alignment of the spots. The ion beam thinning, using a focussed PIPS machine, produces a conventional thin foil, but from a porous precursor. The angle and energy of the beam, Table 1, are controlled to minimise thermal effects and ensure a uniform thinning of the region of interest. Nevertheless a temperature rise is inevitable and this engenders changes in the microstructure. The thinned regions of the foil can be seen to be amorphous but close examination reveals the appearance of lattice images near the edge of the foil over a short range. These can be seen in Fig. 5. The electron diffraction pattern (inset of Fig. 5) shows a continuous ring indicative of a very finely divided crystallised phase and also a diffuse background caused by the remnant amorphous phase. The micrograph in Fig. 6 shows the presence of well crystallised regions of $TiO_2$, in the form of very small crystals, somewhat similar to the appearance of a glass-ceramic. The crystallite size produces a diffraction pattern (inset of Fig. 6) that is made up of many individual spots. Clearly the PIPS treatment has heated up this section of the foil sufficiently to initiate crystallisation. The local temperature could well have reached ~300 °C, since our previous investigation on crystal phase changes [38] formed by annealing of the tubular structure, indicated the appearance of a crystalline phase above 300 °C. Crystalline anodised titania nano-tubes, have been successfully employed in dye sensitised solar cells applications [21].

## Conclusions

Anodised titania nano-tubes have been produced by anodisation of metallic Ti in a fluorine containing electrolyte. A comprehensive TEM investigation of a sample

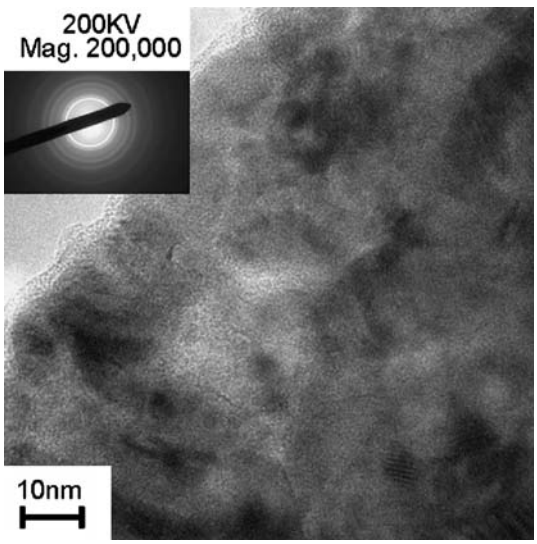


**Fig. 5** PIPS thinned section of the $TiO_2$ anodised film. Lattice images are present near the edge of the foil and the diffraction pattern (inset) indicates the presence of a very finely divided crystalline phase

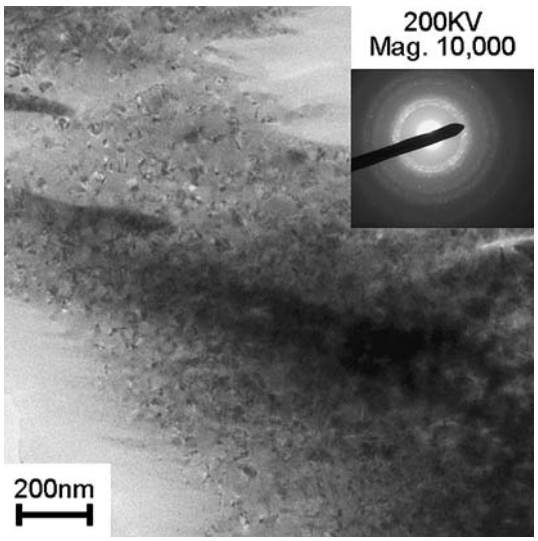


**Fig. 6** Heat affected zone caused by the PIPS thinning process and the corresponding diffraction pattern

anodised for a relatively short period (30 min) combined with information obtained by SEM, provides new insight and helps to explain the formation process of titania nanotubes. In the presence of fluorine ions, a series of interconnected cavities are initially developed which allow current to flow within the oxide/hydroxide film. Results to date suggest that cavities and randomly dispersed pores link up due to the influence of electric field, ion flux and minimisation of surface energy to generate an array of tubes within which the diffusion of ions, electrolyte and water can readily occur. The evolution of oxygen at the anode may also help explain the shape of the tubes which are made up of a stack of rings, produced by collapse of the spherical cavities, This suggests sequential dehydroxylation of the gel at successive stages of the anodisation process. The model discussed explains the structure of the anodic films and suggests how the pore structure develops into nano-tubes. TEM has shown the detailed structure of the film and demonstrated the interconnected porosity. The anodic layer is amorphous, but a slight degree of heating, occurring with Argon ion bombardment, is sufficient to generate crystalline phase.

**Acknowledgements** The Royal Academy of Engineering, The Worshipful Company of Armourers and Brasiers and Novelis are gratefully acknowledged for the financial contribution provided in support of this work. The Nanotechnology Centre of the Cranfield University is also acknowledged for FE-SEM measurements.

## References

1. Zhu X, Kim KH, Jeong Y (2001) Biomaterials 22:2199
2. Yang B, Uchida M, Kim HM, Zhang X, Kokubo T (2004) Biomaterials 25:1003
3. Oh SH, Finõnes RR, Daraio C, Cen LH, Jin S (2005) Biomaterials 26:4938
4. Mor GK, Carvalho MA, Pishko MV, Grimes CA (2004) J Mater Res 19:628
5. Varghese OK, Grimes CA (2003) J Nanosci Nanotechnol 3:277
6. Varghese OK, Gong D, Paulose M, Ong KG, Grimes CA (2003) Sens Actuat B 93:338
7. Varghese OK, Gong D, Paulose M, Ong KG, Dickey EC, Grimes CA (2003) Adv Mater 15:624
8. Fox MA, Dulay MT (1993) Chem Rev 93:341
9. Hoffmann MR, Martin ST, Choi W, Bahnemannt DW (1995) Chem Rev 95:69
10. Mills A, Hill G, Bhopal S, Parkin IP, O'Neill SA (2003) J Photochem Photobiol A: Chem 160:185
11. Mor GK, Shankar K, Varghese OK, Grimes CA (2004) J Mater Res 19:2989
12. Reddy BM, Ganesh I, Khan A (2004) J Mol Catal A: Chem 223:295
13. Jang HD, Kim S-K, Kim S-J (2001) J Nanoparticle Res 3:141
14. Minabe T, Tryk DA, Sawunyama P, Kikuchi Y, Hashimoto K, Fujishima A (2000) J Photochem Photobiol A: Chem 137:53
15. Mor GK, Shankar K, Paulose M, Varghese OK, Grimes CA (2005) Nano Lett 5:191
16. Grätzel M (2003) J Photochem Photobiol C: Photochem Rev 4:145
17. Park JH, Kim S, Bard AJ (2006) Nano Lett 6:24
18. Grätzel M (2001) Nature 414:338
19. Longo C, De Paoli MA (2003) J Braz Chem Soc 14:889
20. Macák JM, Tsuchiya H, Ghicov A, Schmuki P (2005) Electrochem Commun 7:1133
21. Mor GK, Shankar K, Paulose M, Varghese OK, Grimes CA (2006) Nano Lett 6:215
22. Mor GK, Varghese OK, Paulose M, Shankar K, Grimes CA (2006) Sol Energy Mater Sol Cells 90:2011
23. Park N-G, Van de Lagemaat J, Frank AJ (2000) J Phys Chem B 104:8989
24. Wang X, Fujimaki M, Awazu K (2005) Optics Expr 13:1486
25. Zwilling V, Darque-Ceretti E, Boutry-Forveille A, David D, Perrin MY, Aucouturier M (1999) Surf Interface Anal 27:629
26. Macak JM, Sirotna K, Schmuki P (2005) Electrochim Acta 50:3679
27. Gong D, Grimes CA, Varghese OK, Hu W, Singh RS, Chen Z, Dickey EC (2001) J Mater Res 16:3331
28. Taveira LV, Macák JM, Tsuchiya H, Dick LFP, Schmuki P (2005) J Electrochem Soc 152:B405
29. Macak JM, Tsuchiya H, Taveira L, Aldabergerova S, Schmuki P et al (2005) Angew Chem Int Ed 44:7463
30. Paulose M, Shankar K, Yoriya S, Prakasam HE, Varghese OK, Mor GK, Latempa TA, Fitzgerald A, Grimes CA (2006) J Phys Chem B 110:16179
31. Zhao J, Wang X, Chen R, Li L (2005) Solid State Commun 134:705
32. Mor GK, Varghese OK, Paulose M, Mukherjee N, Grimes CA (2003) J Mater Res 18:2588
33. Choi J, Wehrspohn RB, Lee J, Gösele U (2004) Electrochim Acta 49:2645
34. Macak JM, Tsuchiya H, Schmuki P (2005) Angew Chem Int Ed 44:2100
35. Lohrengel MM (1993) Mater Sci Eng R: Report 11:243
36. Rahim MAA (1995) J Appl Electrochem 25:881
37. Cai Q, Paulose M, Varghese OK, Grimes CA (2005) J Mater Res 20:230
38. Regonini D, Bowen CR, Stevens R, Allsopp D, Jaroenworaluck A (accepted) Phys. Status Solidi A